Journal of Cleaner Production 135 (2016) 1054–1064

Contents lists available at ScienceDirect

Journal of Cleaner Production

journal homepage: www.elsevier.com/locate/jclepro

Towards a sustainable paradigm of waste-to-energy process: Enhanced anaerobic digestion of sludge with woody biochar

Yanwen Shen, Jessica L. Linville, Patricia Anne A. Ignacio-de Leon, Robin P. Schoene, Meltem Urgun-Demirtas*

Energy Systems Division, Argonne National Laboratory, 9700 S. Cass Avenue, Lemont, IL 60439, USA

ARTICLE INFO

Article history:
Received 12 March 2016
Received in revised form
11 June 2016
Accepted 24 June 2016
Available online 25 June 2016

Keywords:
Waste-to-energy
Sludge
Biochar
Anaerobic digestion
Mesophilic
Thermophilic

ABSTRACT

This study presents an integrated waste-to-energy process, using two waste streams, sludge generated from the municipal wastewater treatment plants (WWTPs) and biochar generated from the biomass gasification systems, to produce fungible biomethane and nutrient-rich digestate with fertilizer value. Two woody biochar, namely pinewood (PBC) and white oak biochar (WOBC) were used as additives during anaerobic digestion (AD) of WWTP sludge to enhance methane production at mesophilic and thermophilic temperatures. The PBC and WOBC have porous structure, large surface area and desirable chemical properties to be used as AD amendment material to sequester CO_2 from biogas in the digester. The biochar-amended digesters achieved average methane content in biogas of up to 92.3% and 79.0%, corresponding to CO_2 sequestration by up to 66.2% and 32.4% during mesophilic and thermophilic AD, respectively. Biochar addition enhanced process stability by increasing the alkalinity, but inhibitory effects were observed at high dosage. It also alleviated free ammonia inhibition by up to 10.5%. The biochar-amended digesters generated digestate rich in macro- and micronutrients including K (up to 300 m/L), Ca (up to 750 mg/L), Mg (up to 1800 mg/L) and Fe (up to 390 mg/L), making biochar-amended digestate a potential alternative used as agricultural lime fertilizer.

1. Introduction

Waste-to-Energy (WTE) has been a viable waste management strategy in establishing sustainable waste disposal methods and is capable of delivering renewable energy and providing better end products in comparison to other disposal methods. WTE technologies do not only provide renewable source of energy in the form of heat, electricity or fuels from low/negative-value organic waste, but also minimizes environmental pollution because of reduction in volume of organic waste going to landfills and increases the reuse and recycling of disposed materials (Kothari et al., 2010; Stehlík, 2009). The WTE process has many advantages over landfill practices for sustainable waste management. To begin with, this process produces renewable energy efficiently and reduces the national dependence on fossil fuel in an environmental-friendly manner (Brunner and Rechberger, 2015). Furthermore, WTE reduces fugitive greenhouse gas (GHG) emissions from uncontrolled decomposition of organic waste. Reducing methane emission is considered a key strategy in the US government's Climate Action Plan (The White House, 2014). Landfills are the 3rd largest anthropogenic source of methane emission in the US (114.6 MMT CO_2 equivalent), accounting for 18% of the total methane emission in 2013 (US Environmental Protection Agency, 2015). Promoting WTE technology deployment contributes to a further reduction of landfill sites, in such a way that fugitive methane emissions can be reduced. More importantly, the energy generation from WTE process can offset the GHG emissions from waste treatment systems, leading to a carbon-negative economy (Sanchez et al., 2015; Vanholme et al., 2013).

Wastewater treatment plants (WWTPs) in the US produce approximately 7 million tons (dry weight) of sewage sludge per year (Water Environment Research Foundation, 2008), which has a total energy potential of almost 10^5 MJ annually (Shen et al., 2015a).

Anaerobic digestion (AD) is a common technology adopted by the US WWTPs to reduce volume of sludge for disposal. Biogas derived from AD of sludge usually contains 50–70% methane (CH_4), 30–50% carbon dioxides (CO_2) and trace amounts of hydrogen sulfide, ammonia and siloxanes. Upgrading is needed to remove

* Corresponding author.
E-mail address: demirtasmu@anl.gov (M. Urgun-Demirtas).

http://dx.doi.org/10.1016/j.jclepro.2016.06.144
0959-6526/

CO_2 and contaminants and to meet the engine specifications and pipeline standards to be utilized for power generation and renewable vehicle fuel. A range of $0.13–$0.29 per m^3 of methane has been reported for biogas upgrading cost, depending on the system design capacity (100–2000 Nm^3 biogas per hour) and upgrading technology. The biogas upgrading accounts for up to 55% of the overall biomethane production cost (Browne et al., 2011; Petersson and Wellinger, 2009). Therefore, it is necessary to find an efficient alternative to enhance the economy of the onsite biogas utilization for US WWTPs.

During the last two decades the US has witnessed a fast growth of bio-power plants. The annual net electricity generation from the bio-power plants has increased from 45.8 billion kWh in 1990 to 64.3 billion kWh in 2014 (Fig. 1). Woody biomass is the dominant feedstock for the bio-power plants in the US. There are 148 bio-power plants utilizing wood and wood residues to produce 43.1 billion kWh of net power, which counts for two-thirds of the nationwide bio-power production in 2014 (Biomass Magazine, 2015). Biomass gasification is one of the primary technologies used by bio-power plants in the US (US Department of Energy, 2015). Gasification is a thermochemical conversion of carbonaceous material at elevated temperatures (>700 °C) and under oxygen-starved conditions into syngas (80–90%) and biochars and tars (10–20%). Biomass gasifier systems have several advantages, such as high energy efficiency (up to 80% versus10–20% for direct-fired systems), feedstock flexibility (100% biomass versus 5–15% biomass with coal for co-firing systems) and recovery of biochar as high-value co-product. Biochar is a carbonaceous solid with energy density (18 MJ/kg) similar to pulverized coal (Laird et al., 2009). Recently, biochar has attracted a widespread research interest due to its great potential as a soil amendment to improve crop productivity (Chan et al., 2007), enhance carbon sequestration (Woolf et al., 2010) and remediate soil/water contamination (Ahmad et al., 2014).

Biomass gasification is considered as a leading technology for deployment of new bio-power plants in the US over the long term (US Department of Energy, 2015). Under a rapid commercialization scenario, the new gasifier-based bio-power plants could potentially generate biochar on scale of a million tons annually. This estimation is based on the assumption that a 10-MW plant consumes 10 BDT/hr (BDT: bone dry ton) of biomass and that gasifiers yield biochar of up to 10% of the feedstock dry weight (Mohan et al., 2006; Ruiz et al., 2013). Moreover, efficient utilization of biochar may increase the net energy balance of electricity derived from biomass gasification systems and make this process more competitive (Asadullah, 2014; Ruiz et al., 2013).

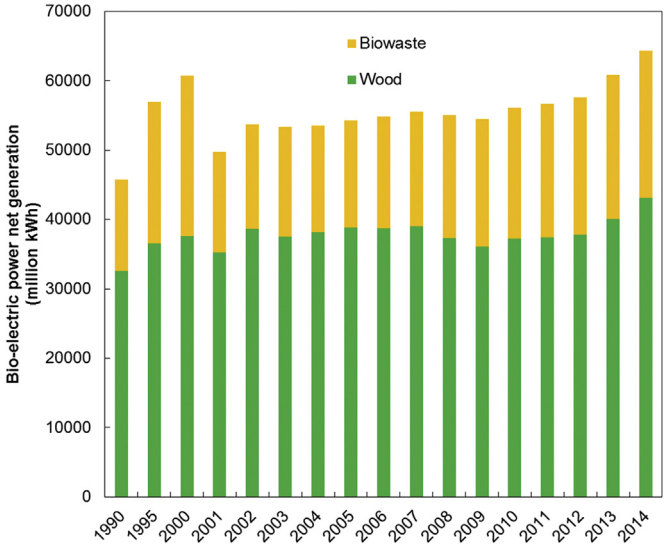

Fig. 1. Net generation of bio-electric power from wood (forest wood, waste wood and logging and mill residues) and biowaste (municipal solid waste, animal manure and agricultural byproducts) in the US, data source: (U.S. Energy Information Administration – Annual Energy Review, 2015).

The concept of using biochar in AD process has emerged recently. Biochar as AD additive was investigated for their capability to alleviate ammonia inhibition (Lu et al., 2016; Luo et al., 2015; Mumme et al., 2014), improve methane yield (Torri and Fabbri, 2014; Zhao et al., 2015) and increase methane content (Shen et al., 2015a,b). However, it should be noted that these experiments were conducted either in syringe reactors (100 mL) (Mumme et al., 2014; Torri and Fabbri, 2014) or using synthetic wastewater (Lu et al., 2016; Luo et al., 2015; Zhao et al., 2015). In the present study, we intend to apply this concept using "real" sludge samples taken from a full-scale WWTP digester at bench-scale reactors (600 mL) to increase production and methane content of biogas.

According to the inventory of the biomass supply in the US (US Department of Energy, 2011), annual production of forestry resources and wastes (e.g. woody biomass) and agricultural resources and residues (e.g. corn stover) are estimated to increase steadily; they represent the major feedstock for bioenergy and bioproducts industry by 2030. We recently reported an enhanced AD system using corn stover biochar as an additive for *in-situ* CO_2 sequestration to simultaneously enhance biomethane production and generate nutrient-enriched digestate (Shen et al., 2015b). Given the significant technical and economic potential of this process, we intend to expand the scope in the present study. Our objective is to develop an integrated WTE process for AD of two waste streams, sewage sludge from WWTPs and woody biochar derived from biomass gasification to produce fungible renewable methane and nutrient-rich soil amendments at different operative temperatures. Two different types of biochar derived from pinewood and white oak were tested, representing softwood and hardwood, respectively among the variety of forestry feedstock used by bio-power plants (Biomass Magazine, 2015). The woody biochars have desirable properties, such as large surface area and chemical stability (Ahmad et al., 2014). The response surface methodology (RSM) is widely adopted for evaluation of AD performance by optimizing multiple parameters (González-Fernández et al., 2011; Jiménez et al., 2014). Therefore RSM was also used in this study to model the response of methane content in biogas and volume of biomethane production to several variables for process scale-up in the future.

2. Materials and methods

2.1. Sewage sludge and biochar

The sludge samples for mesophilic AD experiments were provided by Metropolitan Water Reclamation District of Greater Chicago's Stickney Water Reclamation Plant located in Cicero, IL. The digested (inoculum) and raw (substrate) sludge samples were obtained from outlet and inlet streams of the mesophilic digester (~37 °C), respectively.

The sludge for thermophilic experiments was provided by Woodridge Greene Valley Wastewater Facility located in Woodridge, IL. The facility operates a temperature-phased anaerobic digester system for sludge treatment, consisting of two digesters in sequence in order to separate acid and methane formation stages of the AD process. The first digester (acid phase) is operated at mesophilic temperature (~37 °C) with hydraulic retention time (HRT) of

1.2 days, and the second (methane phase) digester is operated at thermophilic temperature (~53 °C) with HRT of 12 days. The inoculum was obtained from the methane-phase digester while the raw sludge was obtained from the acid-phase digester inlet stream.

The biochar samples were provided by National Renewable Energy Laboratory (NREL) located in Golden, CO. They were derived from gasification of pine and white oak pellets, respectively, using NREL's pilot-scale Thermochemical Process Development Unit (Carpenter et al., 2010).

2.2. Design of anaerobic digestion experiments

The AD experiments were conducted in 600-mL digesters with a working volume of 550 mL at both mesophilic (37 °C ± 1 °C) and thermophilic (55 °C ± 1 °C) temperatures. Both mesophilic and thermophilic AD experiments were conducted at five different test conditions as summarized in Table 1. Test digesters were amended with two dosages of pine biochar (2.49 and 4.97 g/g dry matter of sludge) and white oak biochar (2.20 and 4.40 g/g dry matter of sludge). The rationale for the range of biochar dosage used in this study was provided in Supplementary Materials. Control digesters simulate conventional AD operations in the lab. Each experimental condition was tested in triplicates, with one digester placed in an MPA-200 Biomethane Potential Analyzer system (Challenge Technology, Springdale, AR) and two digesters placed in a New Brunswick's model I24 benchtop incubating shaker (Eppendorf, Hauppauge, NY), otherwise identical continuously stirred digesters. The MPA-200 system consists of an eight-position water bath providing temperature control and agitation, an eight-channel respirometry-based unit for gas measurement, and a computer with pre-installed software for automated gas data recording. Each digester in incubating shaker was attached to a multi-layer foil gas sampling bag (Restek, Bellefonte, PA) for gas collection and the volume of biogas produced was measured using a 100-mL high-performance gastight syringe (Hamilton, Reno, NV) manually on daily basis. The gas volume was adjusted to standard conditions (20 °C, 1 atm) based on the room temperature and pressure recorded daily to account for daily temperature and pressure fluctuations in the lab (Walker et al., 2009). Each digester contained inoculum (4.70 g dry matter), substrate sludge (2.35 g dry matter), biochar (depends on the experimental condition) and deionized water as the makeup water (Table 1). The digesters were sparged with helium gas (99.999% purity, Airgas, IL) for 2.5 min at the beginning of experiments to maintain anaerobic condition. All the experiments were conducted in batch mode and at 50 rpm agitation.

Table 1
Experimental conditions tested for mesophilic and thermophilic anaerobic digestion.

Condition	Ingredients
Control	inoculum[a] + substrate[b]
P250	inoculum + substrate[c] + pine biochar (2.49 g/g dry matter of sludge)
P500	inoculum + substrate + pine biochar (4.97 g/g dry matter of sludge)
WO250	inoculum + substrate + white oak biochar (2.20 g/g dry matter of sludge)
WO500	inoculum + substrate + white oak biochar (4.40 g/g dry matter of sludge)

[a] Sludge collected from the outlet of the WWTP digester.
[b] Primary sludge collected from the inlet of the WWTP digester.
[c] All experimental conditions end up with a 1.25% total solid content of inoculum and substrate sludge.

2.3. Analyses

2.3.1. Biochar characterization

Particle size distribution of the biochar samples was determined by sieving the pre-weighed (10 g) biochar using a micro sieve set (Scienceware, Wayne, NJ). Surface morphology and textural properties of the biochar were characterized by using an FEI Quanta 400F environmental scanning electron microscope (SEM) (FEI, Hillsboro, OR) operated at high vacuum mode at ambient temperature. The biochar sample was mounted on carbon tape and observed under magnifications varying from 200× to 1000× with image captured. Brunauer-Emmet-Teller (BET) surface area, total pore volume and pore size were determined utilizing argon or nitrogen gas adsorption analysis at 77.35 K (Brewer et al., 2009). The pH value of the biochar was measured by mixing 5 g of biochar sample in 100 mL deionized water (Milli-Q, Millipore) stirred at 180 rpm for 24 h at room temperature. Proximate, ultimate and ash elemental analyses were conducted in triplicate using ASTM methods as described previously (Shen et al., 2015b).

2.3.2. Sludge characterization

Total solids (TS) and volatile solids (VS) were determined according to the Standard Methods (APHA et al., 2012). Electrical conductivity (EC) and pH value were measured by using the Oakton PC700 m (Oakton Instruments, Vernon Hills, IL). Chemical oxygen demand (COD), total organic carbon (TOC), total alkalinity (TA), total phosphorus (TP), total nitrogen (TN) and ammonia nitrogen (NH_3-N) were determined using Hach test kits (Hach, Loveland, CO).

2.3.3. Biogas sampling and analysis

Periodically 10 mL of biogas sample was withdrawn from the headspace of each digester and stored in a glass vial (Agilent Technologies, Santa Clara, CA) by using a 10-mL gastight syringe (Hamilton, Reno, NV). Biogas was then analyzed for methane (CH_4) and carbon dioxide (CO_2) content by using a Shimadzu GC-2014 gas chromatograph equipped with a thermal conductivity detector (TCD) and a Supelco 80/100 Porapak Q packed column (5 m × 1/8 inch × 2.1 mm) (Sigma-Aldrich, St. Louis, MO). Helium (99.999% purity, Airgas, IL) was used as the carrier gas. The column temperature was set at 100 °C isothermally and the TCD temperature was set at 170 °C.

2.4. RSM modeling

The RSM modeling was conducted based on the multiple linear regression analysis by using the software program Design Expert 9.0, including an ANOVA for evaluation of the interaction between multiple variables and the response. The detailed procedures were described by Linville et al. (2016) and hence are briefly described herein. The default algorithm picked the best model showing the correlation between the response variables (methane content in biogas and volume of biogas production) and numeric factors (digestion time and biochar dosage). The model terms were manually selected depending on their statistical significance, after which the insignificant terms ($p < 0.05$) were removed except for those required to support the model's hierarchy.

3. Results and discussion

3.1. Biochar characteristics

3.1.1. Physical properties

Fig. 2 shows the particle size distribution of the pine and white oak biochar. About 46.3 wt% of the pine biochar (PBC) particles

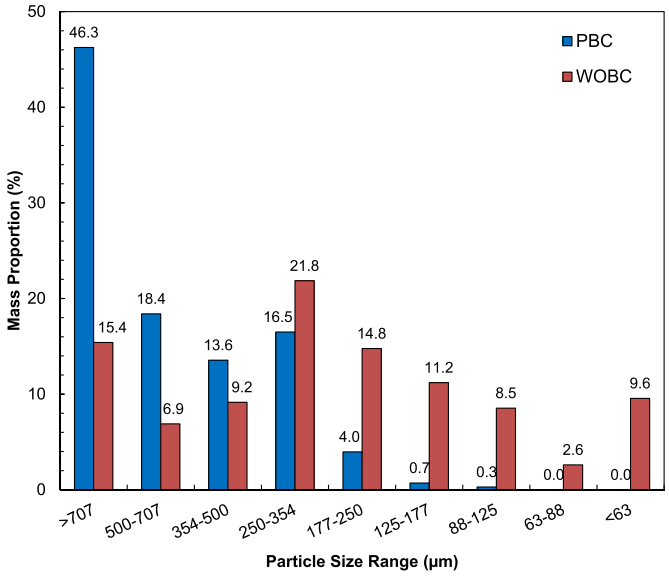

Fig. 2. Particle size distribution of pine (PBC) and white oak biochar (WOBC) samples.

were larger than 707 μm, while the remaining particles ranged from 177 to 707 μm. The white oak biochar (WOBC) had a wide particle size distribution, with the majority of them fall into the size range of 250–354 μm (21.8 wt %). SEM images (Fig. 3A, C) show that both PBC and WOBC consist of irregularly shaped particles with rough surface and highly porous structure. Overall both PBC and WOBC retained the vascular structure similar to their parent woody plant feedstock with disorganized canals arranged side by side. Honeycomb-like porous structures were observed under higher magnification consisting of multiple interconnected networks of micro-, meso- and macro-pores with sizes on order of tens of nanometers to micrometers (Fig. 3B, D). Previous studies have pointed out that pyrolysis/gasification of biomass at high temperature yields biochar with higher porosity (Kim et al., 2012; Sun et al., 2012). Many pores have slit-like narrow opening and macro-pores (>2 nm) appear to account for majority of the pore volume.

Results of the physisorption isotherm analysis are presented in Table 2. The BET surface areas of PBC (310 m^2/g) and WOBC (297 m^2/g) in this study are similar to those of the biochar derived from pyrolysis/gasification of pine or oak wood at temperature ranging from 500 to 700 °C (196–491 m^2/g) (Ahmad et al., 2014; Chen et al., 2008a; Keiluweit et al., 2010). The BET surface area and the pore volume of the biochar are highly dependent on the operational conditions of the thermochemical process. For example, elevated process temperature (Ahmad et al., 2014; Chen et al., 2008a; Keiluweit et al., 2010; Kim et al., 2012) and CO_2 mediated activation treatment (Skodras et al., 2007; Zhang et al., 2004) are highly effective in increasing the BET surface area of the biochar.

3.1.2. Chemical composition

Table 2 presents the chemical composition of the PBC and WOBC. The ash contents of both biochars (PBC 18.7 wt%, WOBC 34.9 wt%) were substantially higher than those of their feedstock (pine pellet 0.3 wt%, oak pellet 0.53 wt%) resulting from the loss of volatile matter and enrichment of the inorganic elements during gasification. The biochars contained up to 1500 times higher concentration of inorganic elements than their corresponding woody biomass feedstocks (data not shown). In comparison of the two biochars, it was observed that WOBC contained approximately 2 times higher concentration of inorganic metal salts (Mg, Fe, Ca, K, Al) than PBC. Silica (SiO_2), magnesium (MgO) and iron (Fe_2O_3) are the three predominant inorganic elements found in PBC and WOBC. The unusually high concentration of Si, Mg and Fe in the biochar might be due to the fact that olivine sand was used as a bedding material in the reactor. Some olivine particles could be occasionally elutriated and mixed with the resultant biochar during gasification (Carpenter et al., 2010; Cheah et al., 2014). On the other hand, agro-plant nutrients, such as N, P and K, were not abundant in PBC or WOBC.

Table 2 also shows that PBC contained lower volatile matter, but higher fixed carbon than that of WOBC. Brewer et al. (2011) reported the positive correlation between fixed carbon fraction (fixed carbon/(fixed carbon + volatiles)) and aromaticity for pyrolysis and gasification biochars. The larger fixed carbon fraction of PBC might indicate its higher aromaticity, which is strongly correlated to the carbon stability and resistance to biodegradation (Zimmerman, 2010). The atomic H/C and O/C ratios illustrated in van Krevelen diagrams are used to estimate the degree of aromaticity and maturation of charcoal (Kookana et al., 2011). The biochar with H/C or O/C ratio less than 0.2 consists predominantly of graphene layers (i.e. planar fused aromatic rings) and is chemically stable (Enders et al., 2012; Kookana et al., 2011; Spokas, 2010). Pyrolysis/gasification reduces oxygen content towards carbon condensation, favorable for carbon-hydrogen bond stretching in the aromatic ring (Chen et al., 2008a). In general, H/C and O/C of biochar decrease with increase of temperature (Ahmad et al., 2012). Both PBC (0.078) and WOBC (0.109) had very low H/C ratios (<0.2), showing their high degree of aromaticity and chemical stability. The extremely low O/C ratio of WOBC (0.051) implies its minimal polarity and high hydrophobicity (Chen et al., 2008a). Enhanced surface hydrophobicity of adsorbent was recently proved as an effective strategy to improve the performance of CO_2 capture in the presence of water (Gao et al., 2015; Nguyen et al., 2014). The reduction of oxygen content is resultant from biomass carbonization, which removes acidic functional groups of the feedstock, thus making the biochar surface become basic (Ahmad et al., 2012). This phenomenon is evidently supported by the fact that the pH value of WOBC (10.15) is slightly higher than that of PBC (9.92). Furthermore, the ash content of WOBC (34.9 wt%) is much higher than that of PBC (18.7 wt%), indicating that biochar pH and ash content are positively correlated, which have been reported previously (Ahmad et al., 2014; Kim et al., 2011; Spokas et al., 2012; Yargicoglu et al., 2015).

In summary, the two woody biochar have favorable characteristics to be applied for CO_2 removal: large surface area, high degree of carbonization, high chemical stability and alkaline pH value. WOBC have higher inorganic salts content along with higher alkalinity, whereas PBC have slightly higher surface porosity. PBC also has significantly higher oxygen content (19.91 wt%) than WOBC (4.05 wt%).

3.2. Bench-scale AD experiments

3.2.1. Biogas and methane production

The time-course profiles of biogas and methane production are shown in Figs. 4 and 5 for mesophilic and thermophilic operation, respectively. The P250 and WO250 ended up with similar cumulative volume of biogas production as the control, while P500 and WO500 produced lower volume of biogas than the control (Figs. 4A and 5A). For both mesophilic and thermophilic operations, all biochar-amended digesters led to higher methane content in the biogas than the control in the sequence of P500 > WO500 > P250 > WO250 > control (Figs. 4B and 5B). The cumulative biogas volume produced during thermophilic AD (825–909 mL) was much higher than that produced during

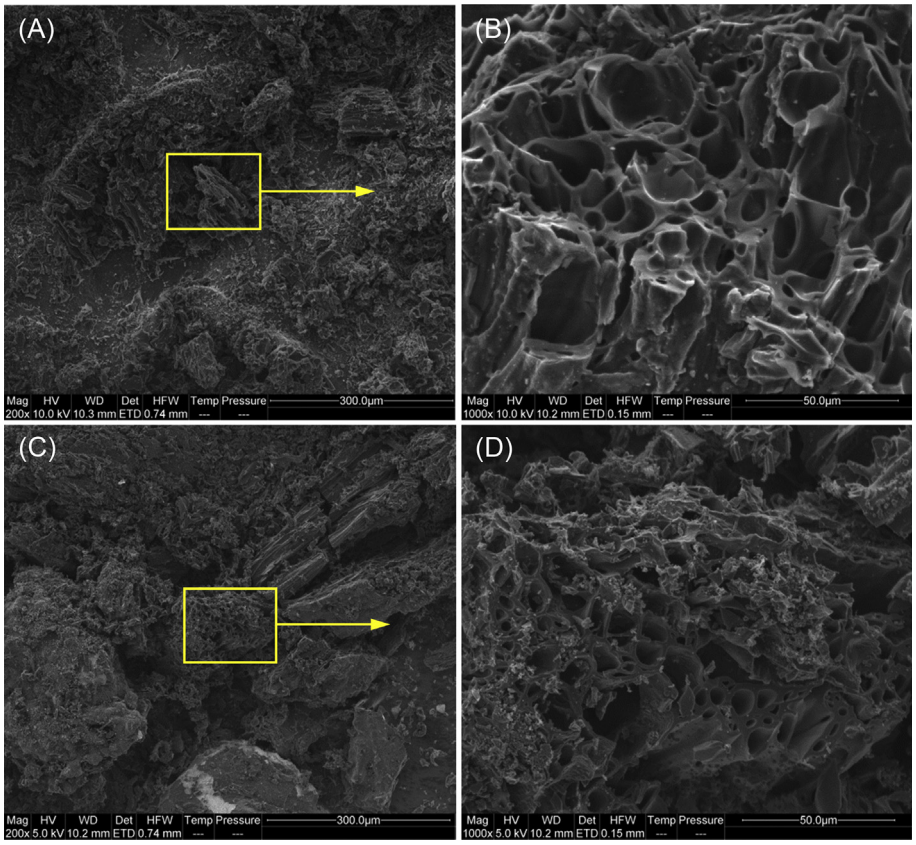

Fig. 3. Scanning Electron Microscope (SEM) images of (A) PBC at 200× magnification; (B) PBC at 1000× magnification; (C) WOBC at 200× magnification; (D) WOBC at 1000× magnification; yellow rectangle shows the zoom-in area. (For interpretation of the references to colour in this figure legend, the reader is referred to the web version of this article.)

Table 2
Physical properties and chemical composition of PBC and WOBC.[a]

Analysis	Parameter (unit)	PBC	WOBC
Physisorption isotherm	BET surface area (m^2/g)	310.19	296.81
	Total pore volume (cm^3/g)	0.19	0.15
	Average pore diameter (nm)	5.07	4.92
Proximate	Moisture (wt %)	0.70 (0.04)	0.82 (0.01)
	Ash (wt %)	18.69 (0.44)	34.90 (0.65)
	Volatile matter (wt %)	3.73 (0.31)	4.58 (0.39)
	Fixed carbon (wt %)	76.22 (1.95)	59.70 (1.02)
Ultimate	C (wt %)	60.04 (1.05)	59.49 (1.24)
	H (wt %)	0.39 (0.04)	0.54 (0.14)
	N (wt %)	0.26 (0.11)	0.18 (0.06)
	O (wt %)	19.91 (0.78)	4.05 (0.69)
	S (ppm)	100 (26)	83 (15)
Atomic ratio	H/C	0.078 (0.009)	0.109 (0.026)
	O/C	0.249 (0.014)	0.051 (0.010)
Ash inorganic elements (mg/g of dry weight)	SiO_2	73.15 (1.88)	141.33 (4.14)
	Al_2O_3	3.20 (0.10)	5.97 (0.72)
	TiO_2	0.03 (0.01)	0.07 (0.00)
	Fe_2O_3	12.54 (0.87)	23.55 (2.53)
	CaO	3.30 (0.44)	7.94 (0.38)
	MgO	83.38 (2.19)	149.99 (3.05)
	Na_2O	0.17 (0.03)	0.17 (0.04)
	K_2O	2.36 (0.23)	4.32 (0.20)
	P_2O_5	0.99 (0.10)	0.44 (0.03)
	SO_3	0.09 (0.05)	0.42 (0.44)
	Cl	0.02 (0.00)	0.03 (0.00)
	CO_2	1.96 (0.32)	4.37 (1.83)

[a] All samples were average values calculated from triplicates, with standard deviation values in parentheses.

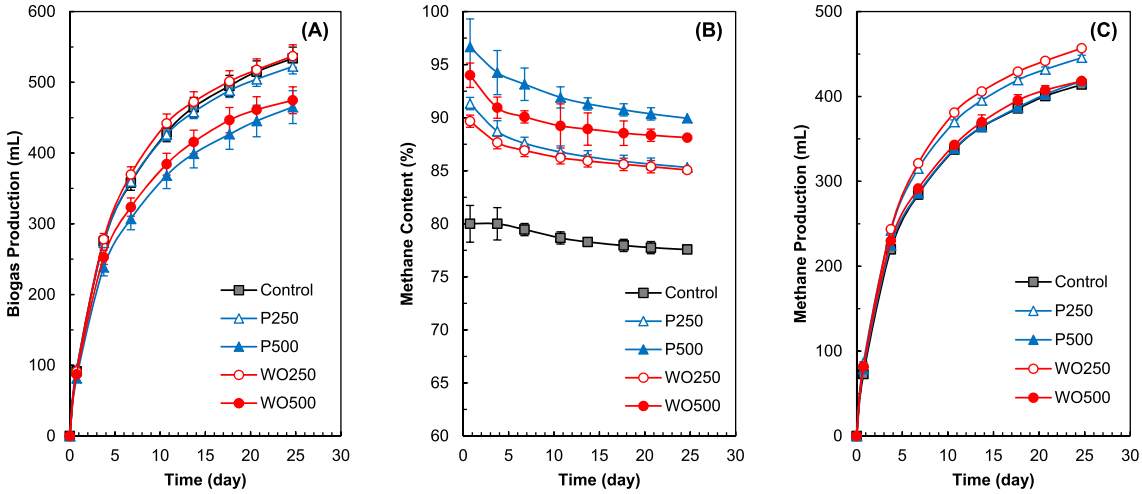

Fig. 4. Time-course profiles of mesophilic anaerobic digestion: (A) cumulative volume of biogas production; (B) methane content in the biogas; (C) cumulative volume of methane production. Data are means of triplicates and error bars show standard deviations.

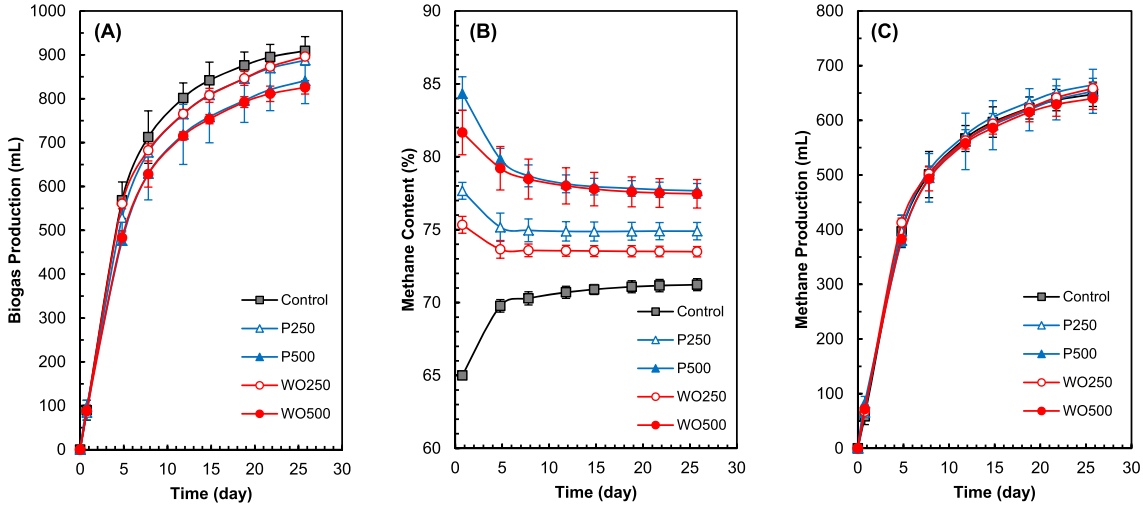

Fig. 5. Time-course profiles of thermophilic anaerobic digestion: (A) cumulative volume of biogas production; (B) methane content in the biogas; (C) cumulative volume of methane production. Data are means of triplicates and error bars show standard deviations.

mesophilic AD (465–537 mL). The difference is attributable to the accelerated reaction rate of AD at thermophilic temperature (Table 3, as discussed later). During mesophilic AD, the methane content in the biogas (CH_4%) from all biochar-amended digesters started from above 90% on day 1 and decreased gradually (Fig. 4B). However, during thermophilic AD, the CH_4% (75.3–84.3%) from the biochar-amended digesters on day 1 were significantly lower ($p < 0.001$) than that observed at mesophilic temperature (89.7–96.7%). Furthermore, the CH_4% from all biochar-amended digesters dramatically dropped from day 1 to day 4 and thereafter retained steady (Fig. 5B). The rate of biogas production may have exceeded the CO_2 sorption uptake rate (Fig. 5A), rendering significantly lower CH_4% of thermophilic digesters.

At mesophilic temperature, the cumulative volume of CH_4

Table 3
Methane yield (Y_{CH_4}), maximum methane production rate ($P_{CH_4,max}$) and reaction rate coefficient (k) for tested AD conditions.

AD condition	Y_{CH_4} (mL CH_4/g COD degraded)	$P_{CH_4,\ max}$ (mL CH_4/day)	k (day^{-1})
Mesophilic-Control	0.305 ± 0.004	72.45 ± 1.11	0.136 ± 0.001
Mesophilic-P250	0.314 ± 0.001	82.90 ± 0.28	0.144 ± 0.001
Mesophilic-P500	0.312 ± 0.006	71.35 ± 1.19	0.132 ± 0.001
Mesophilic-WO250	0.329 ± 0.001	83.22 ± 0.28	0.146 ± 0.002
Mesophilic-WO500	0.318 ± 0.004	79.41 ± 1.27	0.142 ± 0.004
Thermophilic-Control	0.301 ± 0.010	101.84 ± 6.46	0.227 ± 0.004
Thermophilic-P250	0.318 ± 0.006	107.08 ± 3.35	0.230 ± 0.003
Thermophilic-P500	0.307 ± 0.019	103.89 ± 2.81	0.226 ± 0.007
Thermophilic-WO250	0.313 ± 0.004	106.05 ± 3.59	0.226 ± 0.004
Thermophilic-WO500	0.308 ± 0.010	101.50 ± 3.04	0.227 ± 0.011

produced in P250 and WO250 digesters was 7.6–10.3% higher than that of the control ($p < 0.001$) (Fig. 4C); whereas digesters amended with high biochar dosage (P500, WO500) produced similar volume of CH_4 as the control ($p > 0.05$) (Fig. 4C). At thermophilic temperature, only the P250 digester produced significantly higher CH_4 volume (2.68% increase, $p < 0.001$) than the control. However, the increase in CH_4 production was not observed with other biochar-amended digesters. This might result from the lower volume of biogas produced from the biochar-amended digesters compared to the control (Fig. 5A). These results showed that the PBC and WOBC addition can produce biogas with high methane content. The enhancement in CH_4% was more pronounced with mesophilic digesters due to the lower biogas production.

The methane yield and kinetic characteristics of the mesophilic and thermophilic AD were summarized in Table 3. At mesophilic temperature, compared to the control, the biochar amendment raised the methane yield (Y_{CH_4}) by 4.7%, 3.9%, 9.6% and 7.0% of digesters with P250, P500, WO250 and WO500 treatment, respectively. At thermophilic temperature, compared to the control, the biochar amendment raised the Y_{CH_4} by 9.5%, 6.8%, 7.1% and 5.7% of digesters with P250, P500, WO250 and WO500 treatment, respectively. Similar trends were observed with the maximum methane production rate ($P_{CH_4,max}$). The digesters amended with lower biochar dosage (P250, WO250) led to significantly higher Y_{CH_4} values than the control. The *p*-value of each paired test between P250/Control and WO250/Control were 0.002 and 0.002, respectively at mesophilic temperature, and 0.018 and 0.027, respectively at thermophilic temperature. These results were consistent with the CH_4 volume production data. The WO250 digester achieved the maximum cumulative CH_4 volume production (456.8 ± 18.5 mL) with the highest Y_{CH_4} (0.329 ± 0.001 mL CH_4/g COD degraded) and $P_{CH_4,max}$ (83.3 ± 0.3 mL/d) for mesophilic AD, while the P250 digester was the best case for thermophilic AD. Overall, the reaction rate coefficient (*k*) values were higher with thermophilic digesters than those with mesophilic digesters, which was expected due to the faster degradation of sludge at thermophilic temperature (Ge et al., 2011) and higher growth rate of thermophilic methanogens (van Lier et al., 1993). At mesophilic temperature, P250, WO250 and WO500 digesters achieved significantly higher *k*-values (0.142–0.146 d^{-1}) than the control (0.136 d^{-1}). However, no significant differences were observed between any biochar-amended digester and the control with regard to *k*-value at thermophilic temperature ($p > 0.1$ for all conditions). In summary, the above results indicated that microbial activity and kinetics could possibly be inhibited by the high dosage of biochar amendment (P500, WO500).

3.2.2. Digester environment and digestate characteristics

It was expected that the digester pH increased with the biochar addition (Figs. 6A and 7A) because of alkaline nature of biochar samples. For both mesophilic and thermophilic AD, despite the pH drop after the AD of sludge, the biochar-amended digesters maintained the pH in a slightly alkaline range (7.24–7.43 for mesophilic; 7.43–7.61 for thermophilic), significantly higher than that of the control ($p < 0.01$ for all conditions). Furthermore, the total alkalinity concentrations of all biochar-amended digesters increased after AD and they were all significantly higher than those of the control ($p < 0.01$) (Figs. 6B and 7B). This is mainly attributable to the cation release of the alkali and alkaline earth metals (K, Ca and Mg) from the biochar as well as ammonia generation during AD, which can consume CO_2 to generate HCO_3^-/CO_3^{2-} buffer. During mesophilic AD, the biochar addition maintained the total alkalinity in a desirable range (2000–2500 mg $CaCO_3$/L), thus providing the process stability compared to the control with alkalinity dropped during AD (1640 mg $CaCO_3$/L) (Chen et al., 2008b). On the other hand, during thermophilic AD, the control digester started with a desirable alkalinity (2780 mg $CaCO_3$/L). The excessive alkalinity generated by biochar addition may fail to provide stimulatory effects for the AD process. The electrical conductivity (EC) values of the biochar-amended digesters (11.72–20.11 mS cm^{-1}, Figs. 6C, 7C)

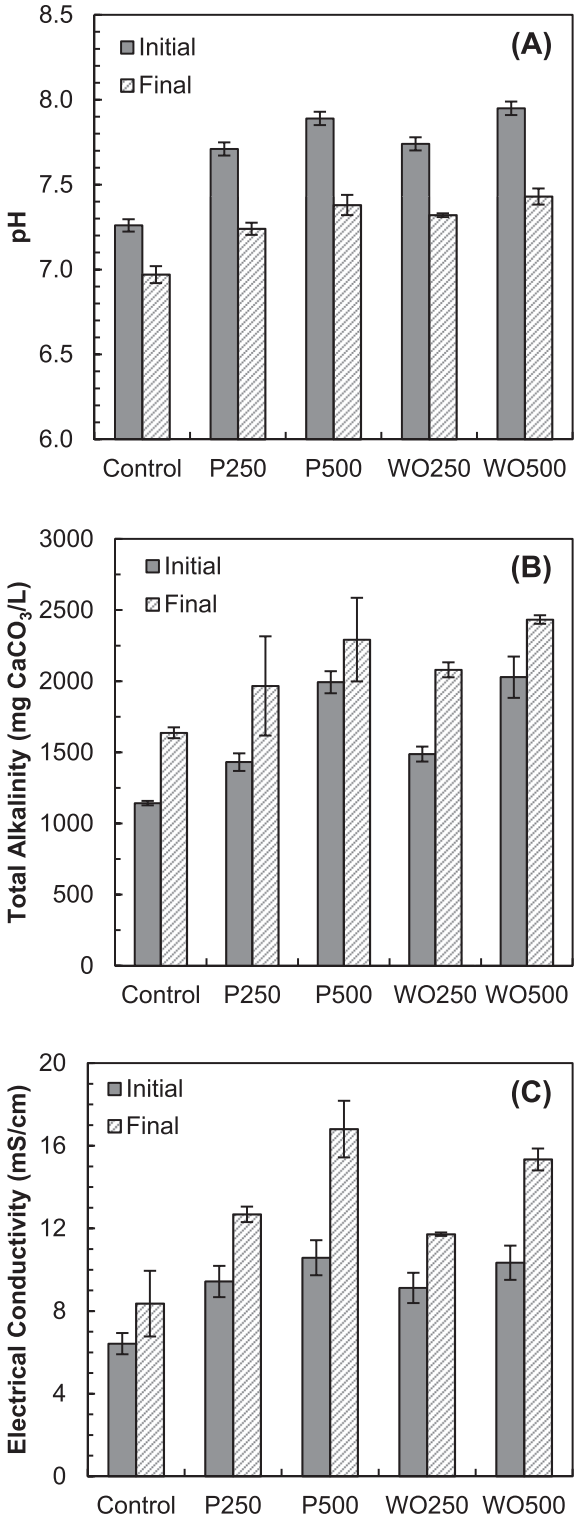

Fig. 6. Digester environment before and after mesophilic anaerobic digestion: (A) pH value; (B) total alkalinity (Total A); (C) electrical conductivity. Data are means of triplicates and error bars show standard deviations.

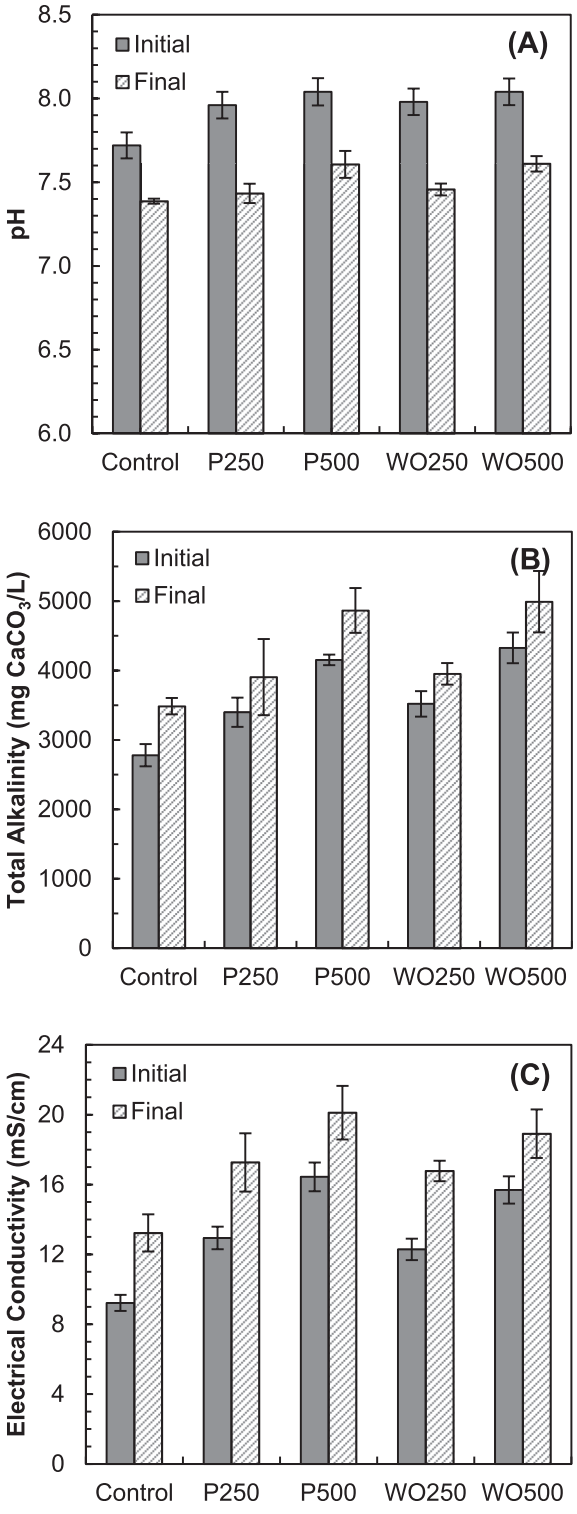

Fig. 7. Digester environment before and after thermophilic anaerobic digestion: (A) pH value; (B) total alkalinity; (C) electrical conductivity. Data are means of triplicates and error bars show standard deviations.

were comparable to those full-scale WWTPs with stable performance (9.97–28.20 mS cm^{-1}) as reported previously (Franke-Whittle et al., 2014). EC is proportional to the ionic concentration in the digester and its measurement can be used to estimate concentration of volatile fatty acids, cations and total alkalinity (Aceves-Lara et al., 2012). Biochar generally possesses conductive properties as a result of its high degree of aromaticity (Bourke et al., 2007). Li et al. (2013) found that the EC of biochar was positively correlated with its fused-ring aromatic structures and aromatic groups. This may support the finding that all biochar-amended digesters showed remarkably higher EC than the control digester regardless of AD temperature. Also, conductive biochar serves as electron mediator to promote direct interspecies electron transfer between the syntrophic acetogen/methanogen communities, thus accelerating methanogenesis (Chen et al., 2014). However, biochar-amended digester with higher EC was not necessarily featured with increased CH_4 production in this study (Figs. 4C and 5C). Biochar is such a complex material that the conductivity-induced stimulatory effects may be counteracted by some unknown toxicity. Therefore, further research will be needed to elucidate those mechanisms.

Fig. S1 shows the TS, VS and COD of the digester slurry before and after AD for all the tested conditions while the COD and VS reductions are elaborated in Table S1. Overall the COD and VS reduction in biochar-amended digesters were comparable to the control. The biochar addition resulted in high TS and VS of the digester slurry (Fig. S1A, B, D, E). Although PBC and WOBC are considered chemically stable and resistant to biodegradation (Spokas, 2010; Zimmerman, 2010), their addition resulted in a significant increase in COD (Fig. S1C, F). It should be noted that the sample is heated at 150 °C for 2 h with H_2SO_4 and a strong oxidizing agent ($K_2Cr_2O_7$) present (APHA et al., 2012). The biochar-amended digesters achieved TOC reduction of 30.1 ± 2.9%, 26.1 ± 7.2%, 28.0 ± 4.6% and 27.2 ± 8.0% with P250, P500, WO250 and WO500 amendment respectively, compared to the control (23.8 ± 6.7%) at mesophilic temperature (Fig. 8A), and of 32.0 ± 3.4%, 36.7 ± 1.5%, 33.0 ± 1.6% and 34.1 ± 2.3% respectively, compared to the control (31.2 ± 3.6%) at thermophilic temperature (Fig. 9A). The biochar addition did not increase the initial TOC in the digester (Figs. 8A and 9A). Notably, biochar amendment enhanced TOC removal, attributing to the increased reaction rate (Table 3). Also, the porous structure of biochar provides a favorable condition for colonization of syntrophic acetogenic bacteria and methanogenic archaea (Xu et al., 2015). Such an interaction would facilitate TOC removal (Luo et al., 2015). The PBC and WOBC addition caused an increase in NH_3-N concentration in the biochar-amended digesters compared to the control regardless of AD temperature initially (Figs. 8B and 9B). This can be attributed to the higher pH (7.71–8.04) with biochar amendment, which would shift the NH_3/NH_4^+ dissociation equilibrium towards free ammonia (NH_3) formation. NH_3 has been postulated as the main cause of toxicity due to its high permeability through cell membranes, which may lead to intracellular proton imbalance and potassium (K^+) depletion (Chen et al., 2008b). NH_3 inhibition is a common problem for thermophilic AD (De la Rubia et al., 2013). A key concern regarding elevated temperatures is the decrease in pK_a of the NH_3/NH_4^+ pair, implying that NH_3 concentration will be much higher for a given pH. Moreover, some thermophilic acetoclastic methanogens are more susceptible to cytotoxic NH_3, (Karakashev et al., 2005; Kato et al., 2014; Sung and Liu, 2003). During thermophilic AD, the NH_3-N concentration increased by 67.0% in the control digester, whereas it fluctuated in the range of −7.2% to 4.7% ($p > 0.1$) in the biochar-amended digesters. This indicated the feasibility of using biochar to alleviate NH_3 inhibition. On the other hand, biochar addition did not lead to any significant increase ($p > 0.05$) of the total nitrogen (Figs. 8C and 9C) or of the total phosphorus concentration in the digester (Figs. 8D and 9D). This is mainly due to the low content of the two elements in the PBC (N = 0.26 ± 0.11%, P_2O_5 = 0.99 ± 0.10 mg/dry g) and WOBC (N = 0.18 ± 0.06%, P_2O_5 = 0.44 ± 0.03 mg/dry g) (Table 2). The K concentration of digestate harvested from biochar-amended digesters increased by 162–367% compared to the control digester (Fig. S2). The digestate was also highly enriched with

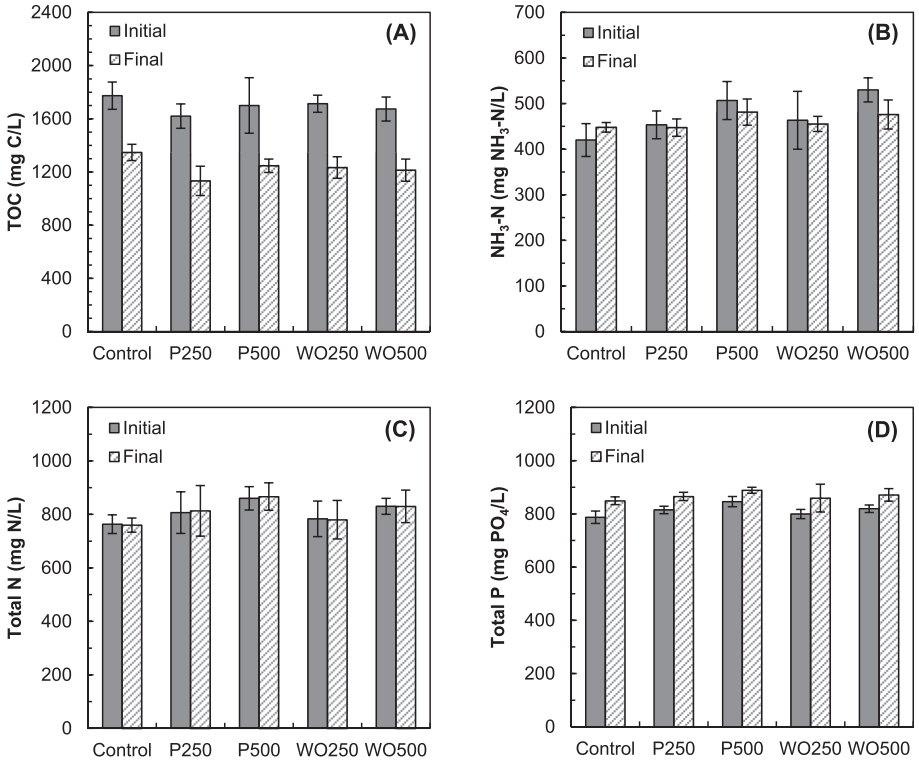

Fig. 8. Sludge characteristics before and after mesophilic anaerobic digestion: (A) total organic carbon (TOC); (B) total ammonia nitrogen (NH_3-N); (C) total nitrogen (total N); (D) total phosphorus (total P). Data are means of triplicates and error bars show standard deviations.

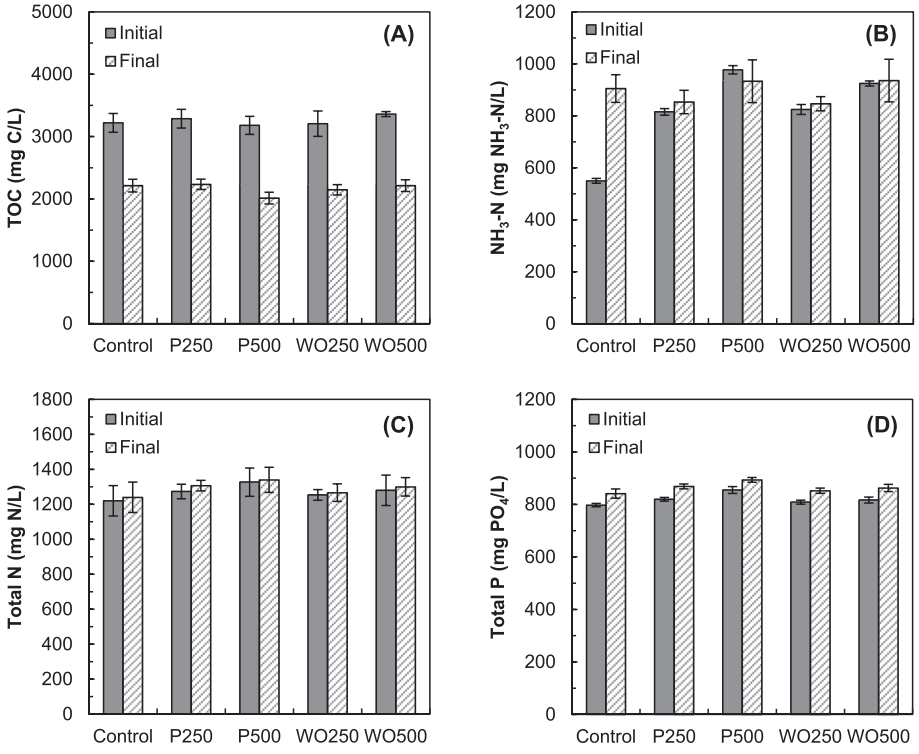

Fig. 9. Sludge characteristics before and after thermophilic anaerobic digestion: (A) total organic carbon (TOC); (B) total ammonia nitrogen (NH_3-N); (C) total nitrogen (total N); (D) total phosphorus (total P). Data are means of triplicates and error bars show standard deviations.

Table 4
Model equations of methane content in biogas (CH_4, %) or volume of methane production (V_{CH_4}, mL) versus digestion time (T, day) and biochar dosage (B, gram per gram of sludge dry matter) for mesophilic and thermophilic AD using response surface methodology (RSM).

Biochar	AD temperature	RSM equation	R^2
PBC	Mesophilic	$CH_4(\%) = 81.169 - 0.363 \cdot T + 4.433 \cdot B - 0.028 \cdot T \cdot B + 0.009 \cdot T^2 - 0.272 \cdot B^2$	0.994
		$V_{CH4}(mL) = 77.043 + 32.728 \cdot T + 22.266 \cdot B - 0.799 \cdot T^2 - 4.375 \cdot B^2$	0.954
WOBC	Mesophilic	$CH_4(\%) = 81.000 - 0.337 \cdot T + 4.860 \cdot B - 0.020 \cdot T \cdot B + 0.009 \cdot T^2 - 0.478 \cdot B^2$	0.990
		$V_{CH4}(mL) = 71.437 + 33.660 \cdot T + 30.846 \cdot B - 0.031 \cdot T \cdot B - 0.827 \cdot T^2 - 6.552 \cdot B^2$	0.953
PBC	Thermophilic	$CH_4(\%) = 68.286 - 0.063 \cdot T + 3.446 \cdot B - 0.077 \cdot T \cdot B + 0.004 \cdot T^2 - 0.121 \cdot B^2$	0.898
		$V_{CH4}(mL) = 80.260 + 58.484 \cdot T + 7.852 \cdot B - 0.028 \cdot T \cdot B - 1.465 \cdot T^2 - 1.532 \cdot B^2$	0.933
WOBC	Thermophilic	$CH_4(\%) = 67.758 - 0.058 \cdot T + 3.885 \cdot B - 0.073 \cdot T \cdot B$	0.924
		$V_{CH4}(mL) = 82.545 + 58.311 \cdot T + 6.649 \cdot B - 0.093 \cdot T \cdot B - 1.465 \cdot T^2 - 1.564 \cdot B^2$	0.925

plant secondary macronutrients (Ca and Mg) and micronutrients (Fe) (Fig. S2), resulting from the high content of these elements in biochar ashes (Table 2). The digestate could also be used in acidic soil (Deal et al., 2012) to displace agricultural lime fertilizer (Laird et al., 2009).

3.3. RSM modeling

The RSM was used to determine the optimal parameters (i.e. digestion time and biochar dosage) for AD experiments with regard to methane content in biogas (CH_4%) and cumulative volume of methane production (V_{CH_4}). As shown in Table 4, quadratic model fits well for most cases except for CH_4% versus WOBC dosage and digestion time during thermophilic AD, which fits the 2-factor-interaction model. The R^2 is in range of 0.898–0.994, indicating the high degree of fit. Based on the weight coefficient of each term, biochar dosage (B) is positively correlated to CH_4% and has the greatest effects on CH_4%. On the other hand, digestion time (T) is negatively correlated to CH_4%. This is consistent with the experimental observations: (1) average CH_4% increased with the biochar dosage (Figs. 4B and 5B); (2) CH_4% slightly decreased in the course of AD (Figs. 4B and 5B). The combined effects of digestion time and biochar dosage ($T{\cdot}B$) have a minimal negative influence on the CH_4%, indicating the weak interaction of the two factors. The digestion time (T) and biochar dosage (B) are positively correlated to the response of V_{CH_4}. The absolute values of biochar dosage's weight coefficient for both of the first-order term (B, positive) and second-order terms (B^2, negative) are higher during thermophilic AD than those during mesophilic AD, indicating the more quantitatively complicated influence of this factor. All of the RSM modeling results were illustrated as three-dimensional (3-D) surface plots in Supplementary Materials (Figs. S2 and S3).

4. Conclusion

This study presented a "one-pot" WTE process aiming to valorize two waste streams (WWTP sludge and gasification woody biochar) in a single step via production of biomethane, *in-situ* CO_2 sequestration and recovery of digestate rich in macronutrients (K, Ca, Mg) and micronutrients (Fe). The two woody biochars tested, pine biochar (PBC) and white oak biochar (WOBC) resulted in average methane content of up to 92.3% and 89.8% in the biogas produced during AD of sludge at mesophilic temperature and of up to 79.0% and 78.5% in the biogas produced at thermophilic temperature, respectively. Correspondingly, the CO_2 sequestration was achieved by up to 66.2% (PBC) and 56.6% (WOBC) during mesophilic AD and up to 32.4% (PBC) and 31.6% (WOBC) during thermophilic AD. Kinetics analysis showed that applying biochar for *in-situ* CO_2 sequestration was more feasible for mesophilic AD because of the slower reaction rate coefficient ($k = 0.132–0.146\ d^{-1}$ for mesophilic versus $k = 0.226–0.230\ d^{-1}$ for thermophilic). Biochar addition enhanced process stability by increasing the alkalinity, but inhibitory effects were observed at high dosage. The biochars also reduced free ammonia formation. Moreover, the biochar-amended digesters generated digestate rich in macro- and micronutrients (K, Ca, Mg) with great potential to be used as agricultural lime fertilizer. Lastly, the quadratic surface models described the response of methane content in biogas and volume of biogas production to digestion time and biochar dosage.

Acknowledgement

This work was sponsored by the Bioenergy Technologies Office in the U.S. Department of Energy Office of Energy Efficiency and Renewable Energy. The submitted manuscript has been created by UChicago Argonne, LLC, Operator of Argonne National Laboratory ("Argonne"). Argonne, a US Department of Energy Office of Science laboratory, is operated under contract no. DE-AC02-06CH11357. The US Government retains for itself, and others acting on its behalf, a paid-up nonexclusive, irrevocable worldwide license in said article to reproduce, prepare derivative works, distribute copies to the public, and perform publicly and display publicly, by or on behalf of the government. The funding source for the work reported here did not have a role in study design, data collection, analysis, data interpretation, writing, or in the decision to publish.

The authors gratefully acknowledge staffs from Metropolitan Water Reclamation District of Greater Chicago's Stickney Water Reclamation Plant and Dupage County's Woodridge Greene Valley Wastewater Facility for their support and assistance.

Appendix A. Supplementary data

Supplementary data related to this article can be found at http://dx.doi.org/10.1016/j.jclepro.2016.06.144.

References

Aceves-Lara, C.A., Latrille, E., Conte, T., Steyer, J.P., 2012. Online estimation of VFA, alkalinity and bicarbonate concentrations by electrical conductivity measurement during anaerobic fermentation. Water Sci. Technol. 65, 1281–1289.
Ahmad, M., Lee, S.S., Dou, X., Mohan, D., Sung, J.K., Yang, J.E., Ok, Y.S., 2012. Effects of pyrolysis temperature on soybean stover- and peanut shell-derived biochar properties and TCE adsorption in water. Bioresour. Technol. 118, 536–544.
Ahmad, M., Rajapaksha, A.U., Lim, J.E., Zhang, M., Bolan, N., Mohan, D., Vithanage, M., Lee, S.S., Ok, Y.S., 2014. Biochar as a sorbent for contaminant management in soil and water: a review. Chemosphere 99, 19–33.
APHA, AWWA, WEF, 2012. Standard Methods for the Examination of Water and Wastewater, twenty-second ed. American Public Health Association; American Water Works Association; Water Environment Federation.
Asadullah, M., 2014. Barriers of commercial power generation using biomass gasification gas: a review. Renew. Sustain. Energy Rev. 29, 201–215.
Biomass Magazine, 2015. List of Biomass Power Plants in the US. Biomass Magazine, Grand Forks, ND.
Bourke, J., Manley-Harris, M., Fushimi, C., Dowaki, K., Nunoura, T., Antal, M.J., 2007. Do all carbonized charcoals have the same structure? 2. A model of the chemical structure of carbonized charcoal. Ind. Eng. Chem. Res. 46, 5954–5967.
Brewer, C.E., Schmidt-Rohr, K., Satrio, J.A., Brown, R.C., 2009. Characterization of biochar from fast pyrolysis and gasification systems. Environ. Prog. Sustain.

Energy 28, 386–396.
Brewer, C.E., Unger, R., Schmidt-Rohr, K., Brown, R.C., 2011. Criteria to select biochars for field studies based on biochar chemical properties. Bioenergy Res. 4, 312–323.
Browne, J., Nizami, A.-S., Thamsiriroj, T., Murphy, J.D., 2011. Assessing the cost of biofuel production with increasing penetration of the transport fuel market: a case study of gaseous biomethane in Ireland. Renew. Sustain. Energy Rev. 15, 4537–4547.
Brunner, P.H., Rechberger, H., 2015. Waste to energy – key element for sustainable waste management. Waste Manag. 37, 3–12.
Carpenter, D.L., Bain, R.L., Davis, R.E., Dutta, A., Feik, C.J., Gaston, K.R., Jablonski, W., Phillips, S.D., Nimlos, M.R., 2010. Pilot-scale gasification of corn stover, switchgrass, wheat straw, and wood: 1. Parametric study and comparison with literature. Ind. Eng. Chem. Res. 49, 1859–1871.
Chan, K.Y., Van Zwieten, L., Meszaros, I., Downie, A., Joseph, S., 2007. Agronomic values of greenwaste biochar as a soil amendment. Aust. J. Soil Res. 45, 629.
Cheah, S., Malone, S.C., Feik, C.J., 2014. Speciation of sulfur in biochar produced from pyrolysis and gasification of oak and corn stover. Environ. Sci. Technol. 48, 8474–8480.
Chen, B., Zhou, D., Zhu, L., 2008a. Transitional adsorption and partition of nonpolar and polar aromatic contaminants by biochars of pine needles with different pyrolytic temperatures. Environ. Sci. Technol. 42, 5137–5143.
Chen, S., Rotaru, A.E., Shrestha, P.M., Malvankar, N.S., Liu, F., Fan, W., Nevin, K.P., Lovley, D.R., 2014. Promoting interspecies electron transfer with biochar. Sci. Rep. 4, 5019.
Chen, Y., Cheng, J.J., Creamer, K.S., 2008b. Inhibition of anaerobic digestion process: a review. Bioresour. Technol. 99, 4044–4064.
De la Rubia, M.A., Riau, V., Raposo, F., Borja, R., 2013. Thermophilic anaerobic digestion of sewage sludge: focus on the influence of the start-up. A review. Crit. Rev. Biotechnol. 33, 448–460.
Deal, C., Brewer, C.E., Brown, R.C., Okure, M.A.E., Amoding, A., 2012. Comparison of kiln-derived and gasifier-derived biochars as soil amendments in the humid tropics. Biomass Bioenergy 37, 161–168.
Enders, A., Hanley, K., Whitman, T., Joseph, S., Lehmann, J., 2012. Characterization of biochars to evaluate recalcitrance and agronomic performance. Bioresour. Technol. 114, 644–653.
Franke-Whittle, I.H., Walter, A., Ebner, C., Insam, H., 2014. Investigation into the effect of high concentrations of volatile fatty acids in anaerobic digestion on methanogenic communities. Waste Manag. 34, 2080–2089.
Gao, F., Li, Y., Bian, Z., Hu, J., Liu, H., 2015. Dynamic hydrophobic hindrance effect of zeolite@zeolitic imidazolate framework composites for CO2 capture in the presence of water. J. Mater Chem. A 3, 8091–8097.
Ge, H., Jensen, P.D., Batstone, D.J., 2011. Temperature phased anaerobic digestion increases apparent hydrolysis rate for waste activated sludge. Water Res. 45, 1597–1606.
González-Fernández, C., Molinuevo-Salces, B., García-González, M.C., 2011. Evaluation of anaerobic codigestion of microalgal biomass and swine manure via response surface methodology. Appl. Energy 88, 3448–3453.
Jiménez, J., Guardia-Puebla, Y., Romero-Romero, O., Cisneros-Ortiz, M.E., Guerra, G., Morgan-Sagastume, J.M., Noyola, A., 2014. Methanogenic activity optimization using the response surface methodology, during the anaerobic co-digestion of agriculture and industrial wastes. Microbial community diversity. Biomass Bioenergy 71, 84–97.
Karakashev, D., Batstone, D.J., Angelidaki, I., 2005. Influence of environmental conditions on methanogenic compositions in anaerobic biogas reactors. Appl. Environ. Microbiol. 71, 331–338.
Kato, S., Sasaki, K., Watanabe, K., Yumoto, I., Kamagata, Y., 2014. Physiological and transcriptomic analyses of the thermophilic, aceticlastic methanogen *Methanosaeta thermophila* responding to ammonia stress. Microbes Environ. 29, 162–167.
Keiluweit, M., Nico, P.S., Johnson, M.G., Kleber, M., 2010. Dynamic molecular structure of plant biomass-derived black carbon (biochar). Environ. Sci. Technol. 44, 1247–1253.
Kim, K.H., Kim, J.Y., Cho, T.S., Choi, J.W., 2012. Influence of pyrolysis temperature on physicochemical properties of biochar obtained from the fast pyrolysis of pitch pine (Pinus rigida). Bioresour. Technol. 118, 158–162.
Kim, P., Johnson, A., Edmunds, C.W., Radosevich, M., Vogt, F., Rials, T.G., Labbé, N., 2011. Surface functionality and carbon structures in lignocellulosic-derived biochars produced by fast pyrolysis. Energy Fuels 25, 4693–4703.
Kookana, R.S., Sarmah, A.K., Van Zwieten, L., Krull, E., Singh, B., 2011. Biochar application to soil: agronomic and environmental benefits and unintended consequences. In: Sparks, D. (Ed.), Advances in Agronomy. Academic Press/Elsevier Inc., San Diego, CA, pp. 103–143.
Kothari, R., Tyagi, V.V., Pathak, A., 2010. Waste-to-energy: a way from renewable energy sources to sustainable development. Renew. Sustain. Energy Rev. 14, 3164–3170.
Laird, D.A., Brown, R.C., Amonette, J.E., Lehmann, J., 2009. Review of the pyrolysis platform for coproducing bio-oil and biochar. Biofuels Bioprod. Biorefin. 3, 547–562.
Li, X., Shen, Q., Zhang, D., Mei, X., Ran, W., Xu, Y., Yu, G., 2013. Functional froups determine biochar properties (pH and EC) as studied by two-dimensional ^{13}C NMR correlation spectroscopy. PLoS One 8, e65949.
Linville, J.L., Shen, Y., Urgun-Demirtas, M., Snyder, S.W., 2016. Effect of particle size and doses of olivine addition on carbon dioxide sequestration during anaerobic digestion of sewage sludge at ambient and mesophilic temperatures. Process Biochem. 51, 59–72.
Lu, F., Luo, C., Shao, L., He, P., 2016. Biochar alleviates combined stress of ammonium and acids by firstly enriching *Methanosaeta* and then *Methanosarcina*. Water Res. 90, 34–43.
Luo, C., Lu, F., Shao, L., He, P., 2015. Application of eco-compatible biochar in anaerobic digestion to relieve acid stress and promote the selective colonization of functional microbes. Water Res. 68, 710–718.
Mohan, D., Pittman, C.U.J., Steele, P.H., 2006. Pyrolysis of wood/biomass for bio-oil: a critical review. Energy Fuels 20, 848–889.
Mumme, J., Srocke, F., Heeg, K., Werner, M., 2014. Use of biochars in anaerobic digestion. Bioresour. Technol. 164, 189–197.
Nguyen, N.T., Furukawa, H., Gandara, F., Nguyen, H.T., Cordova, K.E., Yaghi, O.M., 2014. Selective capture of carbon dioxide under humid conditions by hydrophobic chabazite-type zeolitic imidazolate frameworks. Angew. Chem. Int. Ed. Engl. 53, 10645–10648.
Petersson, A., Wellinger, A., 2009. Biogas Upgrading Technologies – Developments and Innovations. International Energy Agency (IEA) Bioenergy, Paris, France.
Ruiz, J.A., Juárez, M.C., Morales, M.P., Muñoz, P., Mendívil, M.A., 2013. Biomass gasification for electricity generation: review of current technology barriers. Renew. Sustain. Energy Rev. 18, 174–183.
Sanchez, D.L., Nelson, J.H., Johnston, J., Mileva, A., Kammen, D.M., 2015. Biomass enables the transition to a carbon-negative power system across western North America. Nat. Climate Change 5, 230–234.
Shen, Y., Linville, J.L., Urgun-Demirtas, M., Mintz, M.M., Snyder, S.W., 2015a. An overview of biogas production and utilization at full-scale wastewater treatment plants (WWTPs) in the United States: challenges and opportunities towards energy-neutral WWTPs. Renew. Sustain. Energy Rev. 50, 346–362.
Shen, Y., Linville, J.L., Urgun-Demirtas, M., Schoene, R.P., Snyder, S.W., 2015b. Producing pipeline-quality biomethane via anaerobic digestion of sludge amended with corn stover biochar with in-situ CO_2 removal. Appl. Energy 158, 300–309.
Skodras, G., Diamantopoulou, I., Zabaniotou, A., Stavropoulos, G., Sakellaropoulos, G.P., 2007. Enhanced mercury adsorption in activated carbons from biomass materials and waste tires. Fuel Process Technol. 88, 749–758.
Spokas, K., 2010. Review of the stability of biochar in soils: predictability of O: C molar ratios. Carbon Manag. 1, 289–303.
Spokas, K.A., Cantrell, K.B., Novak, J.M., Archer, D.W., Ippolito, J.A., Collins, H.P., Boateng, A.A., Lima, I.M., Lamb, M.C., McAloon, A.J., Lentz, R.D., Nichols, K.A., 2012. Biochar: a synthesis of its agronomic impact beyond carbon sequestration. J. Environ. Qual. 41, 973–989.
Stehlík, P., 2009. Contribution to advances in waste-to-energy technologies. J. Clean. Prod. 17, 919–931.
Sun, H., Hockaday, W.C., Masiello, C.A., Zygourakis, K., 2012. Multiple controls on the chemical and physical structure of biochars. Ind. Eng. Chem. Res. 51, 3587–3597.
Sung, S., Liu, T., 2003. Ammonia inhibition on thermophilic anaerobic digestion. Chemosphere 53, 43–52.
The White House, 2014. Climate Action Plan Strategy to Reduce Methane Emissions (Washington D.C).
Torri, C., Fabbri, D., 2014. Biochar enables anaerobic digestion of aqueous phase from intermediate pyrolysis of biomass. Bioresour. Technol. 172, 335–341.
US Department of Energy, 2011. In: Perlack, R.D., Stokes, B.J. (Eds.), U.S. Billion-ton Update: Biomass Supply for a Bioenergy and Bioproducts Industry. Oak Ridge National Laboratory, Oak Ridge, TN. ORNL/TM-2011/224.
US Department of Energy, 2015. Quadrennial Technology Review 2015, Advancing Clean Electric Power Technologies. U.S. Department of Energy, Washington DC.
US Environmental Protection Agency, 2015. Inventory of U.S. Greenhouse Gas Emissions and Sinks: 1990-2013. US Environmental Protection Agency, Washington DC.
van Lier, J.B., Hulsbeek, J., Stams, A.J.M., Lettinga, G., 1993. Temperature susceptibility of thermophilic methanogenic sludge: implications for reactor start-up and operation. Bioresour. Technol. 43, 227–235.
Vanholme, B., Desmet, T., Ronsse, F., Rabaey, K., Van Breusegem, F., De Mey, M., Soetaert, W., Boerjan, W., 2013. Towards a carbon-negative sustainable bio-based economy. Front. Plant Sci. 4, 174.
Walker, M., Zhang, Y., Heaven, S., Banks, C., 2009. Potential errors in the quantitative evaluation of biogas production in anaerobic digestion processes. Bioresour. Technol. 100, 6339–6346.
Water Environment Research Foundation, 2008. In: Kalogo, Y., Monteith, H. (Eds.), State of Science Report: Energy and Resource Recovery from Sludge. Water Environment Research Foundation, Alexandria, VA.
Woolf, D., Amonette, J.E., Street-Perrott, F.A., Lehmann, J., Joseph, S., 2010. Sustainable biochar to mitigate global climate change. Nat. Commun. 1, 56.
Xu, S., He, C., Luo, L., Lu, F., He, P., Cui, L., 2015. Comparing activated carbon of different particle sizes on enhancing methane generation in upflow anaerobic digester. Bioresour. Technol. 196, 606–612.
Yargicoglu, E.N., Sadasivam, B.Y., Reddy, K.R., Spokas, K., 2015. Physical and chemical characterization of waste wood derived biochars. Waste Manag. 36, 256–268.
Zhang, T., Walawender, W., Fan, L., Fan, M., Daugaard, D., Brown, R., 2004. Preparation of activated carbon from forest and agricultural residues through CO_2 activation. Chem. Eng. J. 105, 53–59.
Zhao, Z., Zhang, Y., Woodard, T.L., Nevin, K.P., Lovley, D.R., 2015. Enhancing syntrophic metabolism in up-flow anaerobic sludge blanket reactors with conductive carbon materials. Bioresour. Technol. 191, 140–145.
Zimmerman, A.R., 2010. Abiotic and microbial oxidation of laboratory-produced black carbon (biochar). Environ. Sci. Technol. 44, 1295–1301.